Academic Sciences International Journal of Pharmacy and Pharmaceutical Sciences

ISSN- 0975-1491 Vol 5, Suppl 2, 2013

Research Article

# CYTOTOXICITY OF PHARMACEUTICALLY OPTIMIZED NANOMETRIC SYSTEMS OF A CHEMOTHERAPEUTIC DRUG ON BREAST AND LIVER TUMOR CELLS

**NOHA M. ZAKI[1#], AHMED ALBARRAQ[2] AND MOHAMED M. HAFEZ[3]**

**[1] Department of Pharmaceutics and Pharmaceutical Technology. College of Pharmacy, Taif University, Taif, KSA, [2] Department of Clinical Pharmacy, College of Pharmacy, Taif University, Taif, KSA [3] Department of Pharmaceutical Microbiology, College of Pharmacy, Taif University, Taif, KSA. Email: drnohazaki@gmail.com**

*Received: 10 Feb 2013, Revised and Accepted: 28 Mar 2013*

**ABSTRACT**

Objective*:* Breast and Liver cancer are widespread among females and males respectively in Kingdom of Saudi Arabia. Nanotechnology is a promising solution for delivery of chemotherapeutic drugs. The present work aims at development and evaluation of passively targeted nanocarrier system of the topoisomerase I inhibitor; Hydroxy Camptothecin (HCPT) chemotherapeutic drug.

Methods*:* To fulfill the above aim, PLGA nanoparticles of HCPT were prepared by the emulsification solvent evaporation technique so as to contain PVA and/or vitamin E derivative (D-α-tocopheryl polyethylene glycol 1000 succinate; TPGS) as emulsifiers. The developed nanoparticles were evaluated for size, zeta potential, morphology, loading and encapsulation efficiency as well as in vitro drug release.

Results: the results revealed that nanoparticles containing TPGS as emulsifier afforded nanoparticles in the desirable nanometric size (< 300 nm) with negative surface charge and high HCPT encapsulation efficiency (>70%). The Differential Scanning Calorimetric (DSC) thermograms revealed that HCPT is incorporated in the nanoparticles in an amorphous state while TEM revealed a nanometer size range, a characteristic round shape and a monodisperse nature of the nanoparticles. The in-vitro release profile depicted an initial burst release of HCPT from the nanoparticles followed by a sustained release profile. The Cytotoxicity of the nanoparticles was measured in MCF7 (human breast adenocarcinoma cell line) and HEpG2 (human hepatocellular carcinoma cells) visually, by trypan blue exclusion test and by MTT assay. The HCPT nanoparticles containing TPGS lowered the IC50 and improved the cytotoxicity as compared to simple HCPT solution. ***Conclusion:*** PLGA/TPGS nanoparticles of HCPT potentiate its anticancer effect and hence provide a promising nanosystem in breast and liver chemotherapy.

**Keywords:** breast cancer, liver cancer, PLGA nanoparticles, cytotoxicity, chemotherapeutic drugs.

## INTRODUCTION

Cancer is common in Saudi Arabia [1, 2] ; according to GLOBOCAN 2008, the most common type among females is breast cancer[1]; representing 24% of all cancer cases according to the National cancer registry and GLOBOCAN 2008 [2, 3] with around 8000 cases discovered each year. On the other hand, liver cancer is one of the most common causes of cancer in males [1, 4]. Chemotherapy is an imperative therapeutic approach for the treatment of these types of cancer. The selective increase in tumor tissue uptake of anticancer agents would be of great interest in cancer chemotherapy since many anticancer drugs are effluxed by cancer cells. In the context of tumor biology, it is known that the tumor vasculature is leaky and possesses an enhanced capacity for the uptake of macromolecules and colloidal drug carriers of up to 400nm [5-8]. This effect is known as the enhanced permeability and retention (EPR) effect. There is a great interest in "**Nanotechnology**" for the targeted treatment of cancer through the delivery of conventional anticancer agents via nanoparticulate drug carriers known as "nanoparticles"[9, 10]. Nanoparticles can accumulate at the tumor site as a result of the EPR effect (passive targeting mechanism) [11]. The objectives of the present work are to apply pharmaceutical nanotechnology for chemotherapy and undergo cytotoxicity studies for establishment of efficacy of nanotechnology biomaterials.

Camptothecin (CPT), a cytotoxic alkaloid first isolated from Camptotheca acuminata, is a promising antitumor agent that targets the nuclear enzyme topoisomerase I (Top I) and inhibits the relegation of the cleaved DNA strand, which leads to the death of tumor cells[12]. Camptothecin and its more potent analogue 10-hydroxycamptothecin (HCPT) have demonstrated their antitumor activity toward a wide range of experimental tumors. However, poor solubility in water and in physiological acceptable organic solvents limits their practical use[13]. Among the many ways to solve the solubility problem associated with the delivery of water-insoluble CPTs, the polymeric nanoparticulate drug delivery system might be one of the simplest and most promising in terms of drug loading capacity, formulation stability, biocompatibility and the 'passive' targeting ability[14].

A paramount concern was to link tumor biology with physicochemical aspects of nanotechnology for formulation of optimized biocompatible HCPT - loaded nanoparticles with improved efficacy against breast and liver cancer. Hence, we used biodegradable polymers as safe and biocompatible delivery vehicles for HCPT. By appropriate design, nanoparticles may act to target tumor tissues or cells, protecting the drug from efflux transporter proteins. The right parameters for formulating stable nanoparticles using novel surfactants/stabilizers (which inhibit P-glycoprotein efflux) will be undertaken and the cytotoxicity of these nanosystems will be evaluated on cancer cell line namely MCF7 (human breast adenocarcinoma cell line) and HEpG2 (human hepatocellular liver carcinoma cells).

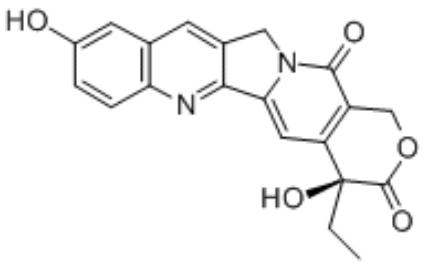


10- Hydroxycamptothecin (HCPT)

## MATERIALS AND METHODS

### Materials

10-Hydroxy camptothecin (HCPT) was purchased from QINGDAO GREEN-EXTRACT BIOLOGY AND TECHNOLOGY CO.,LTD, Qingdao, China. Poly lactide-co- glycolide (PLGA) (lactide:glycolide ) 50:50, carboxylate end group; inherent viscosity, 0.18 dL/g; Mw, 4000 Da) was a kind gift from Purac Biochem (Netherlands). Polyvinyl alcohol

(Mw 6,000 Da) was purchased from Sigma. D-α-tocopheryl polyethylene glycol 1000 succinate (vitamin E TPGS or simply, TPGS) was purchased from Sigma. Dimethyl sulfoxide (DMSO) was purchased from Sigma.

**Cell Culture**

MCF7 (human breast adenocarcinoma cell line) and HEpG2 (human hepatocellular liver carcinoma cells) (ECACC, UK) were maintained as, respectively adherent cell cultures at 37°C in a humidified atmosphere (5% CO2) in Dulbecco modified Eagle's minimal essential medium (DMEM, 25 mM glucose) supplemented with 2 mM glutamine (Gibco) and 10% heat-inactivated fetal calf serum (FCS) (Invitrogen, UK). Antibiotic solution composed of 100 IU/ml penicillin and 100 IU/ml streptomycin (Gibco) was added to the culture medium during cell maintenance. For monolayer formation, The cells were detached using trypsin–EDTA (Invitrogen, UK) consisting of 2.5% (w/v) of trypsin and 0.2% (w/v) EDTA in PBS. The cells were suspended in DMEM containing FCS to a count of $10^5$ living cells/ml as determined by trypan blue exclusion stain and a hemocytometer. For cytotoxicity and, cellular uptake experiments, aliquots of the cells were seeded in 96-well plates and incubated till confluency.

**Methods**

**Preparation of HCPT-loaded PLGA nanoparticles**

Nanoparticles were prepared by emulsification-solvent evaporation method as previously reported [15]. One ml solution of HCPT in dichloromethane (DCM) was used (1mg/ml) and added to PLGA solution in DCM (50mg/ml) and vortex mixed. The previous organic phase was then added to 50 ml aqueous solution of PVA (0.5% or 1%)[16] or TPGS (0.03% or 0.1%) [15, 17] and homogenized using high shear homogenizer at 48,000 rpm. The organic phase was then evaporated on a magnetic stirrer at room temperature.

**Table1: Composition and formula code for HCPT nanoparticles**

| Formula code | | PLGA (50:50) acid terminated | | |
|---|---|---|---|---|
| | | Drug: polymer ratio | 1:25 | 1:50 |
| | PVA | 0.5% | 1 | 2 |
| | | 1% | 3 | 4 |
| | TPGS | 0.03% | 5 | 6 |
| | | 0.1% | 7 | 8 |

**Morphological examination of nanoparticles**

Morphological examination of the nanoparticles was conducted using (TEM) transmission electron microscope JEM-100S (Japan). One drop of nanoparticles suspension was placed on a copper grid covered with nitrocellulose membrane and air-dried before staining with phosphotungstic acid solution (1%) or uranyl acetate solution (0.1%).

**Measurement of nanoparticle size and particle size distribution**

The mean particle size of the nanoparticles, the particle size distribution (measured as the polydispersity index (PDI) and zeta potential were determined by Dynamic light scattering method using a ZataNanosizer (Malvern, ver. 6.12).

**Determination of nanoparticles yield,**

Nanoparticles yield was determined gravimetrically by Eq. (1).

Nanoparticles Yield (%) = weight of nanoparticles/ weight of the feeding polymer and drug X 100 **Eq.1**

**Determination of HCPT loading content and encapsulation efficiency of nanoparticles**

The encapsulation efficiency (and loading efficiency), were determined as reported previously [18]. Briefly, the amount of HCPT unencapsulated in the nanoparticles (after centrifugation of the nanoparticles at 7000 rpm for 1h) was deducted from the initial amount of drug added as compared to the amount used in the encapsulation process (or certain weight of nanoparticles for LC ), by Eq.2& 3 respectively. The amount was calculated spectrophotometrically using a pre-constructed calibration curve y = 0.061x+0.044 ($R^2$=0.995). The calibration curve was obtained using a stock solution of HCPT (2.6 mg/ml in DMSO; and serial dilutions in 2% Tween 80 in water). The absorbance of the different concentrations (1.3-20.8µg/ml) was measured at $\lambda_{max}$ 382 nm.

Encapsulation efficiency (EE%) = (Initial amount of HCPT used - Amount of HCPT unencapsulated) / Initial amount of HCPT usedX100 **Eq.2**

Loading Capacity (LC%) = (Initial amount of HCPT used in formulation - Amount of HCPT unencapsulated) / weight of nanoparticles X 100 **Eq.3**

**In vitro release of HCPT- loaded nanoparticles**

In vitro release of HCPT from the nanoparticles was evaluated using a dialysis bag diffusion technique on freshly prepared HCPT nanoparticles [19]. The nanoparticle solutions were firstly dispersed in distilled water to have a diluted nanoparticles dispersion. An aliquot of 2 ml of the drug-loaded NPs was transferred to a glass cylinder having the length of 10 cm and diameter of 2.5 cm fitted with a dialysis membrane with 12000 MWCO (Sigma, USA) presoaked in distilled water. The cylinder was placed in a receiving compartment containing 100 ml distilled water containing 2% tween 80 to maintain sink condition with gentle agitation in a shaking water bath. Periodically, 5 ml of the release medium was with-drawn assayed spectrophotometrically at 382 nm. Samples withdrawn were replaced by the same volume of fresh medium dissolution medium. The experiments were done in triplicates.

**Cellular Uptake Studies by Fluorescent Microscopy**

The cellular uptake was performed using MCF7 and HEpG2 cells. The visualization study was done using a fluorescent microscope as previously described [20, 21]. Briefly, the cells were seeded on sterile poly-L-lysine-coated coverslips placed in six-well plates and placed in the incubator at 37°C to allow cell attachment. To each well, 250 µl of nanoparticles dispersion was added, and the plates were incubated for 30 min in a humid atmosphere at 37°C in a CO2 incubator. Immediately after removal of the colloidal dispersion by gentle aspiration, 1 ml trypan blue solution was incubated with the cells for 1 min after which the cells were rinsed at least four times with pre-warmed PBS pH 7.4. Cell fixation and permeabilization was achieved by dipping in 4% formaldehyde solution for 20 min at room temperature followed by 0.05% Triton X-100 in PBS for 5 min in order to allow actin staining using Texas-red phalloidin (Molecular probes, The Netherlands). At the same time, the cells were incubated for 3 min with 200 nM4',6-diamidino-2-phenylindole (DAPI) solution in PBS for nuclear staining followed by rinsing. The coverslips were carefully inverted onto a drop of mounting liquid on a microscopic slide and stored in the dark at 4°C. For visualization using confocal microscopy, Fl-NPs were excited using a 488-nm laser, and its emission was read from 497 to 560 nm (green emission) while excitation at 358 nm induces DAPI fluorescence and its emission was read from 450 to 468 nm (blue emission). For further image processing, ImageJ® Software was used.

**Cytotoxicity Studies**

For measurement of cytotoxicity on HCPT-NPs, the MTT colorimetric assay was used [22-24]. Briefly, MCF7 and HEpG2 cells were diluted with culture medium to a count of 1×105 cells/ml and seeded in 96-well micro-titer plate at density of 10,000 cells/well. At the time of each experiment, the culture medium was removed and replaced with 100 µl HCPT solution (free drug dissolved in DMSO), NPs-

encapsulated HCPT dispersions (equivalent to HCPT dose 10-1200 ng/mL). Cells incubated with culture medium served as negative control) while cells incubated with plain NPs (unmedicated) were used to determine cytotoxicity due to NPs formulation per se. The cells were incubated for 48 h at 37°C in a humid atmosphere with 5% CO2, then the test dispersion was removed by gentle aspiration and the cells were rinsed three times with pre-warmed pH 7.4 PBS. Subsequently, a 100 µl of 0.5 mg/ml of MTT reagent in DMEM (3-[4,5-dimethylthiazol-2-yl]-3,5-diphenyl tetrazolium bromide dye) was added to each well, and the plates were incubated for 4 h after which the stain was removed. To solubilize the formazan crystals, a 100 µl of sterile DMSO was added to each well, and the plates were shaken for 5 min [22]. Finally, the absorbance (A) was measured at 550 nm in a micro-titer plate reader (TECAN Safire, Tecan Austria GmbH, Grödig, Austria). The cell cytotoxicity was calculated using the following equation [23, 25]:

$$\text{Cell Cytotoxicity (\%)} = A_{test}/A_{control} \times 100$$

Where $A_{test}$ is the absorbance of the cells incubated with the NPs dispersions and $A_{control}$ is the absorbance of the cells incubated with the culture medium only (negative control). IC50, the drug concentration at which reduction of 50% cell viability occurs in comparison with that of the control sample, is calculated by the curve fitting of the cell viability data [26, 27].

**Statistical Analysis**

All tests were conducted in triplicate, and the results were expressed as the mean ± standard deviation. Statistical analysis of the data was performed using one-way analysis of variance (ANOVA) followed by the Bonferroni test for multiple comparison at $P<0.05$ using Instat-ANOVA software.

**RESULTS & DISCUSSION**

**Preparation of 10-HydroxyCamptothecin-PLGA Nanoparticles**

Topoisomerase inhibitors belonging to the camptothecins family have renowned potent chemotherapeutic effect [14, 28]. Nevertheless, the camptothecins have a major weakness of undergoing hydrolysis at physiological pH leading to drug inactivation and clinical ineffectiveness [12, 29]. 10-Hydroxy camptothecin (HCPT) is an analogue of camptothecin with a hydrolysis half-life of 21 min. The hydrolytic reaction of HCPT is a reversible pH-sensitive interconversion from the potent lactone form (stable below pH 5) to the poorly active carboxylate form (stable above pH 8). It has been previously reported that PLGA polymers can provide an acidic microclimate [30] which can serve in controlling the stability of encapsulated substances for numerous molecules [31, 32]. Previously reported that PLGA microspheres stabilized 10-HCPT for more than 10 weeks (>95% lactone) under a simulated physiological milieu due to an acidic micro environment that stabilizes the lactone form of 10- HCPT[33]. In another mechanistic study, the degradation of vincristin in PLGA occurred through acid-catalyzed loss of the N-formyl group that was completely inhibited by neutralization of acidic microclimate of PLGA [31]. The yield of nanoparticles was 82% which was satisfactory.

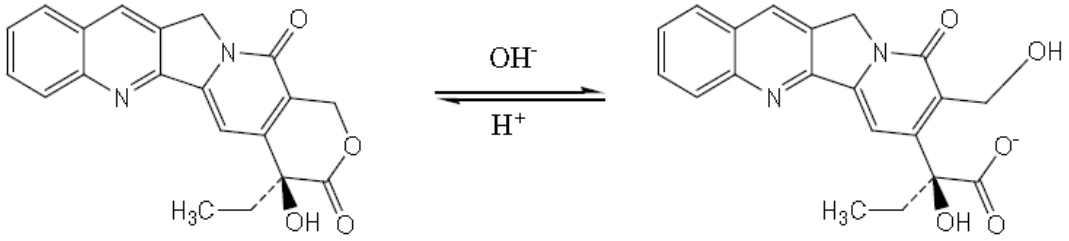


**Lactone form (active)** **Carboxylate form (inactive)**

**Characterization of HCPT Nanoparticles**

Regarding nanoparticles sizes, charge (zeta potential) and encapsulation efficiency of HCPT, results are shown in Table 3 the formulations (F6, F7 and F8) had the lowest particle size. Regarding the nanoparticles surface charge, table (3) reveal that PLGA NPs prepared with PVA (F1-F4) initially possessed a negative charge as indicated by a negative zeta potential value (range from -14.3 to -22.5 mV). The NPs additionally containing TPGS (F5-F8) emulsifiers maintained this negative zeta potential. This might be attributed to the carboxylate end group on the acid terminated PLGA polymer. These results are in agreement with those previously reported [15, 19, 34].

**Table 2: Particle Size, zeta potential, EE and LC of HCPT-PLGA nanoparticles**

| Formula Code | Particle Size (nm)± S.D. | Zeta potential (mV)± S.D. | EE (%) ± S.D. | LC (%) ± S.D. |
|---|---|---|---|---|
| 1 | 690 ± 6 | -14.3 ± 2.1 | 67.2 ± 1.8 | 35.3 ± 2.4 |
| 2 | 450 ± 8 | -16.7 ± 3.1 | 69.5 ± 3.1 | 23.5 ± 3.2 |
| 3 | 315 ± 7 | -21.7 ± 2.3 | 68.33 ± 2.5 | 28.3 ± 2.5 |
| 4 | 318 ± 5 | -15.9 ± 2.2 | 71.2 ± 2.1 | 31.1 ± 2.9 |
| 5 | 303 ± 4 | -18.6 ± 2.3 | 73.2 ± 3.8 | 29.5 ± 5.2 |
| 6 | 264 ± 8 | -17.8 ± 2.4 | 70.2 ± 2.8 | 32.2 ± 4.6 |
| 7 | 138 ± 7 | -22.5 ± 4.1 | 77.4 ± 2.4 | 35.8 ± 2.3 |
| 8 | 182 ± 8 | -21.2 ± 3.3 | 79.34 ± 4.2 | 34.1 ± 2.7 |

Regarding the effect of emulsifier type on the nanoparticles characteristics, It is noteworthy that NPs prepared by emulsification- solvent evaporation using 0.1% TPGS as emulsifier exhibited smaller size and higher encapsulation efficiency (>70%) than other NPs prepared by emulsification- solvent evaporation. These results are in accordance with those reported previously[17, 35, 36]. Indeed, TPGS being a potent emulsifier by virtue of its bulky structure and large surface area, is recommended for nanoparticles formulation of anticancer drugs providing higher emulsification effect, higher drug encapsulation efficiency, and better therapeutic effects[37]. The size distribution of the developed nanoparticles was narrow and mono-modal as shown in figures 1 and 2 for formulas F7 and F8 respectively. As shown, the developed NPs that have small particle size (below 200 nm) is chosen since our target was to optimize nanoparticles preparative conditions to achieve passive targeting for tumor cells. Indeed, a narrow particle size distribution is an important aspect in passive targeting of nanoparticles as well as for stability issues [34].

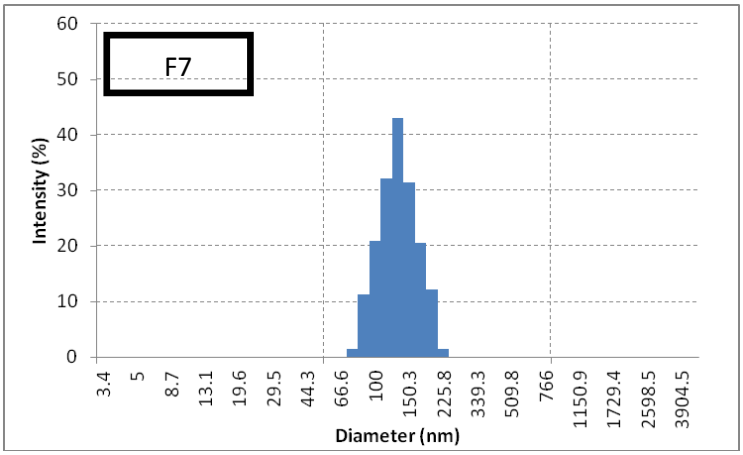


**Fig. 1: Size distribution of HCPT-PLGA nanoparticles F7.**

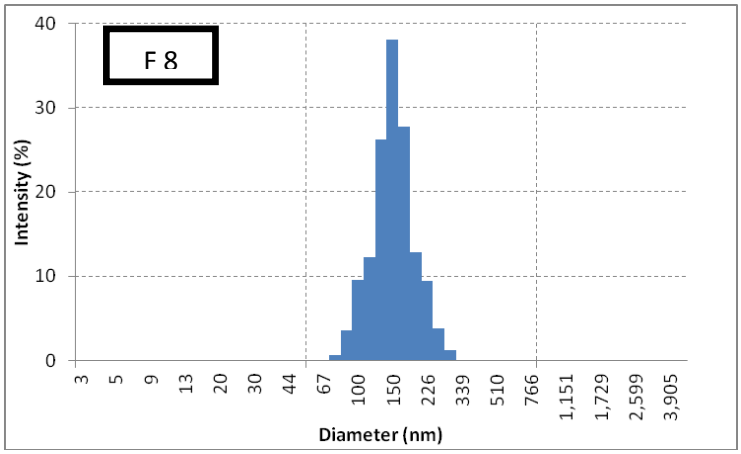


**Fig. 2: Size distribution of HCPT-PLGA nanoparticles F8.**

The morphology of the prepared nanoparticles was revealed by Transmission Electron Microscopic (TEM) images for nanoparticles F7 (fig. 3). From the images, it is obvious that PLGA Nanoparticles were in the nanometer range, had a characteristic round shape and were monodisperse, Similar results are reported by Parveen and Sahao [38] and Chung et al.[39] and others [40, 41]

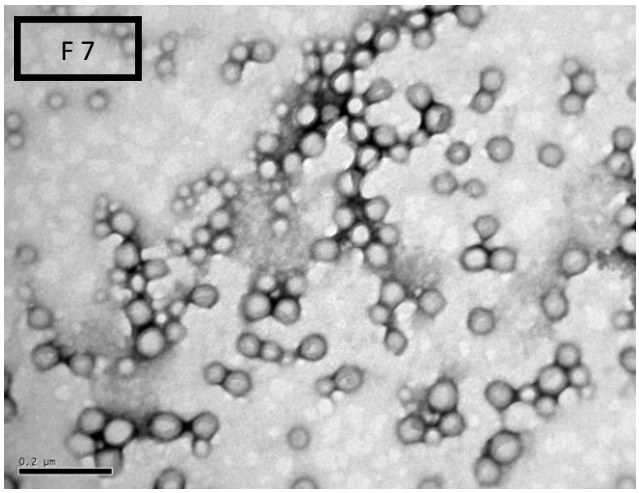


**Fig. 3: TEM images for HCPT-PLGA nanoparticles (F7)**

The DSC thermograms corresponding to HCPT ,PLGA, and HCPT-PLGA nanoparticles are shown in Fig. 4. The PLGA thermogram displayed an endothermic peak at 45 °C, corresponding to the polymer transition temperature (Tg). The DSC curve of HCPT showed a single melting peak at about 267 °C and started to degrade as it melted. No HCPT melting peak was visible in the case of drug loaded nanoparticles. This might be attributed to the amorphous state of the drug dispersed in the nanoparticles. Since there was no change in the Tg of the polymer, it can be concluded that there is almost no interaction between the drug and the polymer. Simailar results were obtained but with 9-nitrocamptothecin in PLGA nanoparticles[18].

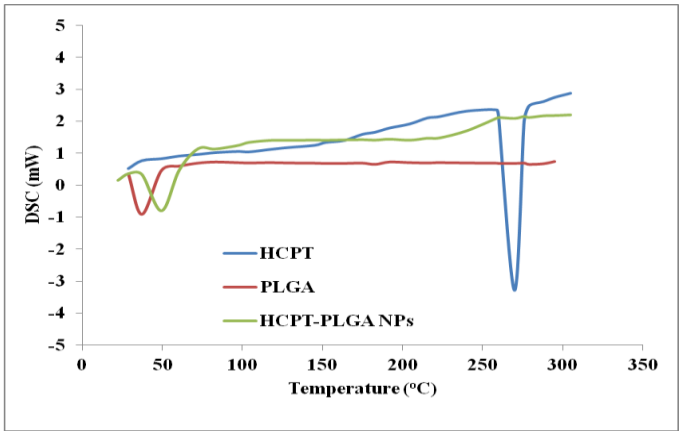


**Fig. 4: Differential scanning calorimetry (DSC) thermograms of HCPT, PLGA and HCPT- PLGA nanoparticles (F7)**

**In vitro release of HCPT from developed nanoparticles**

The release of HCPT from the different PLGA nanoparticles was performed in PBS containing surfactant to simulate physiological milieu [42] and maintain sink condition. Release profiles are shown in Fig. 5. It was revealed that all nanoparticles exhibited a burst drug release where about 20-60% of drug was released over a period of 2h, followed by a distinct prolonged release up to more than 30h that could be attributed to diffusion of the dissolved drug within the PLGA core of the nanoparticles into the dissolution medium. This release behavior is characteristic of PLGA nanoparticles and has been extensively reported [43-46] and considered as a limitation of PLGA nanoparticles. As shown in Fig. 5, the drug release in F7 and F8 exhibited reduced burst effect. Overall in vitro release data indicate that HCPT -PLGA nanoparticles F7, was capable of sustaining HCPT release rate with relatively low burst release. This formula was selected for further studies on breast and liver cancer cell lines.

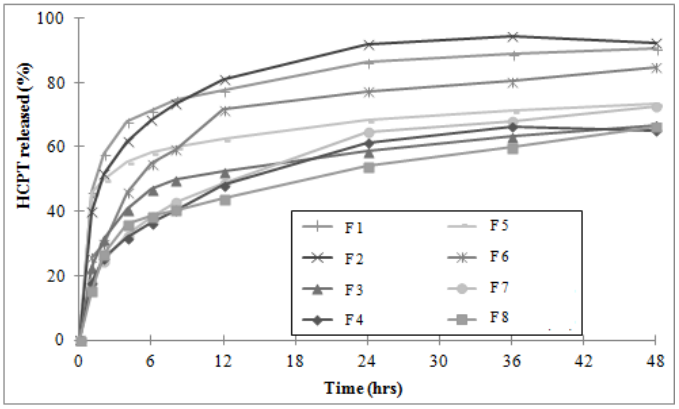


**Fig. 5: In vitro release of HCPT from PLGA nanoparticles (F1–F8) in PBS containing 1% tween 80 at 37°C.**

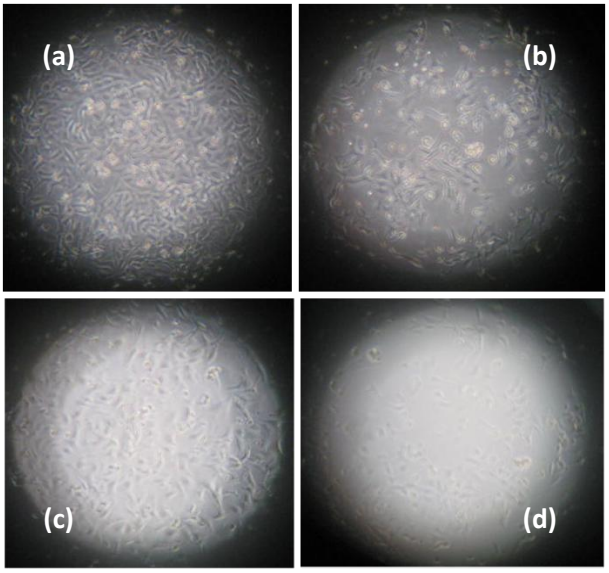


**Fig. 6: Light microscopic images (inverted microscope) showing cytotoxicity of MCF-7 cells upon incubation with HCPT- PLGA Nanoparticles at 0 time (a), 4h (b), 10 h (c) and 24h (d).**

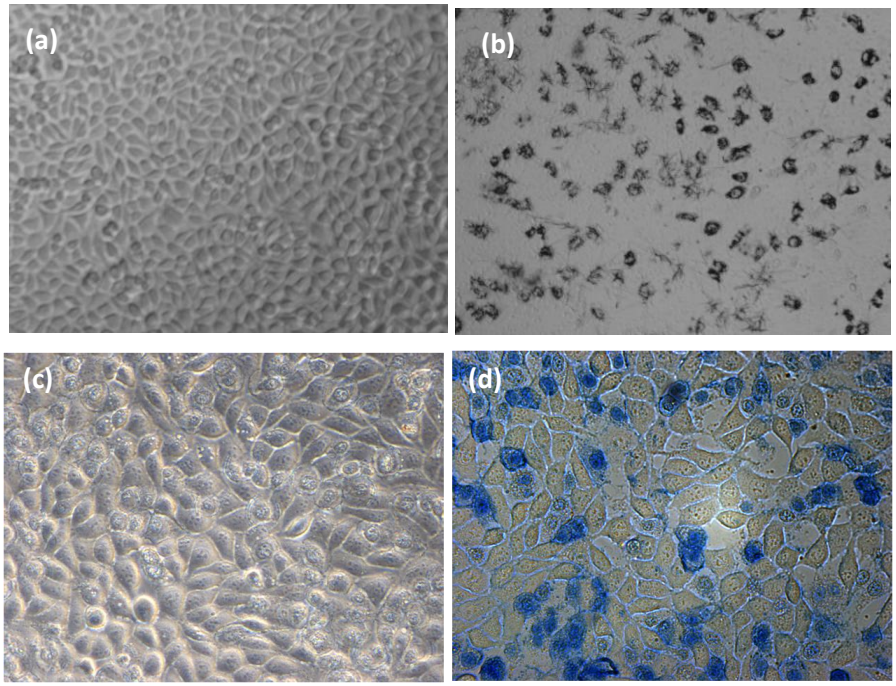


**Fig. 7: Light microscopic images (inverted microscope) showing the cytotoxic effect of HCPT-PLGA Nanoparticles; F7 incubated with human liver carcinoma cells (HEpG-2).**

HEpG2 Cells incubated with HCPT Nanoparticles at 0 time (a) and 24 h (b). HEpG2 Cells incubated with HCPT Nanoparticles (c) were stained blue due to intracellular diffusion of trypan blue dye at 12 h (d)

**Cytotoxicity of HCPT nanoparticles to cancer cell lines**

Preliminary assessment of the cytotoxicity of HCPT nanoparticles to cancer cell lines was done by visualization of the cells incubated with HCPT-NPs using an inverted microscope. Fig. 6 and fig. 7 show the toxic effect observed following incubation of nanoparticles formulation with MCF7 and HEpG2 respectively.

The in vitro cytotoxicity of different HCPT-loaded PLGA nanoparticles was investigated and compared with that of the simple HCPT solution using human breast cancer cells MCF7 and human liver cancer cells HEpG2. As a negative control, empty NPs were used. Cells were treated with the same concentrations of free or NPs-encapsulated HCPT. After 2 days in the presence of NPs formulations, cells were analyzed for their survival using the MTT colorimetric assay for the dehydrogenase activity of viable cell. In both cell lines (Fig. 8), HCPT encapsulated NPs demonstrated a significantly superior cytotoxicity compared to that of the free drug; this might be attributed to the nanoparticles-mediated intracellular delivery of the topoisomerase I inhibitor HCPT and the bypass of the efflux mechanism experienced by free drug solution. Indeed, the $IC_{50}$ value towards MCF7 cells was 859 ng/ml for free HCPT while it was 505 ng/ml for HCPT-NPs containing TPGS (F7) i.e. $IC_{50}$ lowered by ~40%. Statistical analysis revealed that these values were significantly different ($P < 0.05$). Towards HEpG2 cells, the $IC_{50}$ values were 1053 ng/ml for free HCPT and 408 ng/ml for HCPT- NPs/TPGS (F7). Statistical analysis revealed that these values were significantly different ($P < 0.05$).

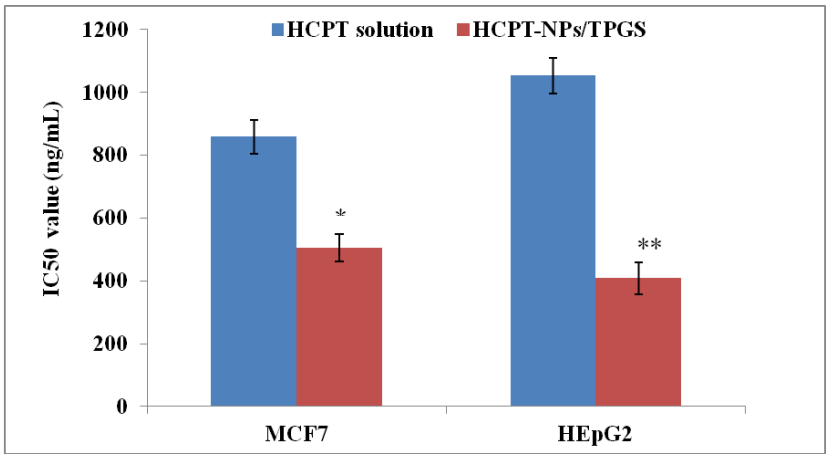


**Fig. 8: The $IC_{50}$ values of HCPT NPs (F7) in MCF7 and HEpG2 cells.**

*, ** significantly different from HCPT solution in MCF7 and HEpG2 cells respectively at $P < 0.05$ using one-way ANOVA followed by Bonferroni test for multiple comparison.

The improved cytotoxicity might be explained by the increased stability of the cytotoxic lactone form of HCPT inside the PLGA NPs core due to the acidic microclimate this polymer present [31, 33, 47], and better uptake of HCPT-containing NPs by the cells either as a result of inhibition of efflux mechanism in cancer cells by TPGS [48]. The highest cytotoxicity (revealed by the lower IC50) observed in

the two cell lines could be explained by the previously reported cytotoxic effect of TPGS specifically against cancer cells and not against normal cells where it acts as a pro-apoptotic agent against cancer cells [49-54]. Moreover, TPGS has been demonstrated to enhance cellular uptake of NPs and thus increase the cancer cell mortality [36]. The co-administration of TPGS could enhance cytotoxicity by inhibition of P-glycoprotein-mediated multi-drug resistance, and hence increase the oral absorption and bioavailability of anticancer drugs as previously reported [15, 27, 34, 48, 55]. TPGS per se has demonstrated significant cytotoxic effect [56] and hence it could provide a synergistic anticancer action with HCPT.

To confirm the uptake of nanoparticles by the cells and their internalization, fluorescent PLGA nanoparticles were incubated with HEpG2 cells. Figure 9 shows that the intracellular localization of the nanoparticles (green fluorescent spots) inside the cells (red for actin filaments existing just below cell membrane; blue for nucleus). These results suggest that cytotoxic effect is mediated by internalization of nanoparticles and subsequent release of the anticancer drug intracellularly and not the simple diffusion of HCPT through cell membrane [57]. These results are in agreement with those previously reported on camptothecin analogues in different nanocarriers [58-60] and other anticancer drugs [61-63]

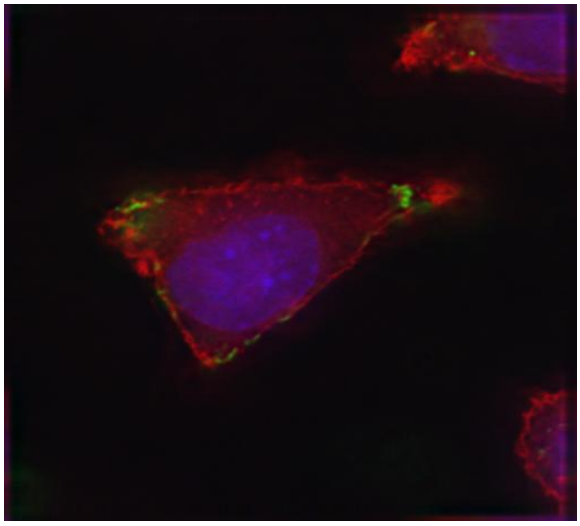

**Fig. 9: Fluorescent microscopic images showing internalization and cellular uptake of FA-PLGA nanoparticles (green fluorescence) by HEpG2 human liver adenocarcinoma cells (red fluorescence) following incubation of nanoparticles with the cells for 24h**

## CONCLUSION

We optimized different parameters for nanoparticles preparation and evaluated them pre-clinically on MCF7 and HEpG2 cancer cell lines. The optimized nanoparticles containing TPGS proved more cytotoxic to cancer cells than simple free HCPT solution. Hence, nanoparticles of acid terminated PLGA polymer and HCPT with powerful TPGS emulsifier can be used to effectively deliver high payloads of HCPT to breast and liver cancer cells.

## REFERENCES

1. Ajarim DS. Cancer at king khalid university hospital, riyadh. Ann Saudi Med 1992:12(1):76-82.
2. http://globocan.iarc.fr/factsheet.asp#KEY.
3. http://appserv.kfshrc.edu.sa/default/health/disease/3?Language=English.
4. http://globocan.iarc.fr/factsheet.asp#MEN.
5. Davaran S, Rashidi MR, Pourabbas B, Dadashzadeh M, Haghshenas NM. Adriamycin release from poly(lactide-coglycolide)-polyethylene glycol nanoparticles: synthesis, and in vitro characterization. Int J Nanomedicine 2006:1(4):535-539.
6. Yu JM, Li YJ, Qiu LY, Jin Y. Polymeric nanoparticles of cholesterol-modified glycol chitosan for doxorubicin delivery: preparation and in-vitro and in-vivo characterization. J Pharm Pharmacol 2009:61(6):713-719.
7. Gu F, Langer R, Farokhzad OC. Formulation/preparation of functionalized nanoparticles for in vivo targeted drug delivery. Methods Mol Biol 2009:544:589-598.
8. Gindy ME, Prud'homme RK. Multifunctional nanoparticles for imaging, delivery and targeting in cancer therapy. Expert Opin Drug Deliv 2009:6(8):865-878.
9. Mahor A, Alok S, Gupta Y, Jain SK. Body distribution and stability studies on mitoxantrone loaded solid lipid nanoparticles conjugated with concanavalin-A. Int J Pharm Pharm Sci 2010:2(2):39-42.
10. Shaji J, Jain V. Solid lipid nanoparticles: a novel carrier for chemtherapy. Int J Pharm Pharm Sci 2010:2(3):8-17.
11. Kumari A, Yadav SK, Yadav SC. Biodegradable polymeric nanoparticles based drug delivery systems. Colloids Surf B Biointerfaces 2009.
12. Hatefi A, Amsden B. Camptothecin delivery methods. Pharm Res 2002:19(10):1389-1399.
13. Hofheinz RD, Gnad-Vogt SU, Beyer U, Hochhaus A. Liposomal encapsulated anti-cancer drugs. Anticancer Drugs 2005:16(7):691-707.
14. Kehrer DF, Soepenberg O, Loos WJ, Verweij J, Sparreboom A. Modulation of camptothecin analogs in the treatment of cancer: a review. Anticancer Drugs 2001:12(2):89-105.
15. Zhang Z, Feng SS. Nanoparticles of poly(lactide)/vitamin E TPGS copolymer for cancer chemotherapy: synthesis, formulation, characterization and in vitro drug release. Biomaterials 2006:27(2):262-270.
16. Cohen-Sela E, Teitlboim S, Chorny M, Koroukhov N, Danenberg HD, Gao J, Golomb G. Single and double emulsion manufacturing techniques of an amphiphilic drug in PLGA nanoparticles: formulations of mithramycin and bioactivity. J Pharm Sci 2009:98(4):1452-1462.
17. Feng SS, Zeng W, Teng Lim Y, Zhao L, Yin Win K, Oakley R, Hin Teoh S, Hang Lee RC, Pan S. Vitamin E TPGS-emulsified poly(lactic-co-glycolic acid) nanoparticles for cardiovascular restenosis treatment. Nanomed 2007:2(3):333-344.
18. Derakhshandeh K, Erfan M, Dadashzadeh S. Encapsulation of 9-nitrocamptothecin, a novel anticancer drug, in biodegradable nanoparticles: factorial design, characterization and release kinetics. Eur J Pharm Biopharm 2007:66(1):34-41.
19. Betancourt T, Brown B, Brannon-Peppas L. Doxorubicin-loaded PLGA nanoparticles by nanoprecipitation: preparation, characterization and in vitro evaluation. Nanomed 2007:2(2):219-232.
20. Zaki NM, Nasti A, Tirelli N. Nanocarriers for cytoplasmic delivery: cellular uptake and intracellular fate of chitosan and hyaluronic acid-coated chitosan nanoparticles in a phagocytic cell model. Macromol Biosci 2011:11(12):1747-1760.
21. Zaki NM, Tirelli N. Assessment of nanomaterials cytotoxicity and internalization. Methods Mol Biol 2011:695:243-259.
22. Mosmann T. Rapid colorimetric assay for cellular growth and survival: application to proliferation and cytotoxicity assays. J Immunol Methods 1983:65((1-2)):55-63.
23. Devi JS, Bhimba BV, Ratnam K. In vitro anticancer activity of silver nanoparticles synthesized using the extract of Gelidiella Sp. . Int J Pharm Pharm Sci 2012:4 (suppl 4):710-715.
24. Zaki NM, Hafez MM. Enhanced antibacterial effect of ceftriaxone sodium-loaded chitosan nanoparticles against intracellular Salmonella typhimurium. AAPS PharmSciTech 2012:13(2):411-421.
25. Nasti A, Zaki NM, de Leonardis P, Ungphaiboon S, Sansongsak P, Rimoli MG, Tirelli N. Chitosan/TPP and chitosan/TPP-hyaluronic acid nanoparticles: systematic optimisation of the preparative process and preliminary biological evaluation. Pharm Res 2009:26(8):1918-1930.
26. Lou H, Zhang X, Gao L, Feng F, Wang J, Wei X, Yu Z, Zhang D, Zhang Q. In vitro and in vivo antitumor activity of oridonin nanosuspension. Int J Pharm 2009:379(1):181-186.
27. Zhang Z, Huey Lee S, Feng SS. Folate-decorated poly(lactide-co-glycolide)-vitamin E TPGS nanoparticles for targeted drug delivery. Biomaterials 2007:28(10):1889-1899.

28. Zunino F, Dallavalleb S, Laccabuea D, Berettaa G, Merlinib L, Pratesi G. Current status and perspectives in the development of camptothecins. Curr Pharm Des 2002:8(27):2505-2520.
29. Garcia-Carbonero R, Supko JG. Current perspectives on the clinical experience, pharmacology, and continued development of the camptothecins. Clin Cancer Res 2002:8(3):641-661.
30. Shenderova A, Burke TG, Schwendeman SP. The acidic microclimate in poly(lactide-co-glycolide) microspheres stabilizes camptothecins. Pharm Res 1999:16(2):241-248.
31. Marinina J, Shenderova A, Mallery SR, Schwendeman SP. Stabilization of vinca alkaloids encapsulated in poly(lactide-coglycolide) microspheres. Pharm Res 2000:17(6):677-683.
32. Cuong NV, Hsieh MF, Huang CM. Recent development in nano-sized dosage forms of plant alkaloid camptothecin-derived drugs. Recent Pat Anticancer Drug Discov 2009:4(3):254-261.
33. Shenderova A, Burke TG, Schwendeman SP. Stabilization of 10-hydroxycamptothecin in poly(lactide-co-glycolide) microsphere delivery vehicles. Pharm Res 1997:14(10):1406-1414.
34. Feng SS, Mu L, Win KY, Huang G. Nanoparticles of biodegradable polymers for clinical administration of paclitaxel. Curr Med Chem 2004:11(4):413-424.
35. Xie J, Wang CH. Self-assembled biodegradable nanoparticles developed by direct dialysis for the delivery of paclitaxel. Pharm Res 2005:22(12):2079-2090.
36. Mu L, Feng SS. A novel controlled release formulation for the anticancer drug paclitaxel (Taxol): PLGA nanoparticles containing vitamin E TPGS. J Control Release 2003:86(1):33-48.
37. Pan J, Feng SS. Targeted delivery of paclitaxel using folate-decorated poly(lactide)-vitamin E TPGS nanoparticles. Biomaterials 2008:29(17):2663-2672.
38. Parveen S, Sahoo SK. Long circulating chitosan/PEG blended PLGA nanoparticle for tumor drug delivery. European Journal of Pharmacology 2011:670(2â€“3):372-383.
39. Chung TW, Wang SS, Tsai WJ. Accelerating thrombolysis with chitosan-coated plasminogen activators encapsulated in poly-(lactide-co-glycolide) (PLGA) nanoparticles. Biomaterials 2008:29(2):228-237.
40. Bilensoy E, Sarisozen C, Esendagli G, Dogan AL, Aktas Y, Sen M, Mungan NA. Intravesical cationic nanoparticles of chitosan and polycaprolactone for the delivery of Mitomycin C to bladder tumors. Int J Pharm 2009:371(1-2):170-176.
41. Nafee N, Taetz S, Schneider M, Schaefer UF, Lehr CM. Chitosan-coated PLGA nanoparticles for DNA/RNA delivery: effect of the formulation parameters on complexation and transfection of antisense oligonucleotides. Nanomedicine 2007:3(3):173-183.
42. Zaki NM, Artursson P, Bergstrom CA. A modified physiological BCS for prediction of intestinal absorption in drug discovery. Mol Pharm 2010:7(5):1478-1487.
43. Danhier F, Lecouturier N, Vroman B, Jerome C, Marchand-Brynaert J, Feron O, Preat V. Paclitaxel-loaded PEGylated PLGA-based nanoparticles: in vitro and in vivo evaluation. J Control Release 2009:133(1):11-17.
44. Shu S, Zhang X, Teng D, Wang Z, Li C. Polyelectrolyte nanoparticles based on water-soluble chitosan-poly(L-aspartic acid)-polyethylene glycol for controlled protein release. Carbohydr Res 2009:344(10):1197-1204.
45. Basarkar A, Devineni D, Palaniappan R, Singh J. Preparation, characterization, cytotoxicity and transfection efficiency of poly(DL-lactide-co-glycolide) and poly(DL-lactic acid) cationic nanoparticles for controlled delivery of plasmid DNA. Int J Pharm 2007:343(1-2):247-254.
46. Pillai RR, Somayaji SN, Rabinovich M, Hudson MC, Gonsalves KE. Nafcillin-loaded PLGA nanoparticles for treatment of osteomyelitis. Biomed Mater 2008:3(3):034114.
47. Shenderova A, Burke TG, Schwendeman SP. The acidic microclimate in poly(lactide-co-glycolide) microspheres stabilizes camptothecins. Pharm Res 1999:16(2):241-248.
48. Johnson BM, Charman WN, Porter CJ. An in vitro examination of the impact of polyethylene glycol 400, Pluronic P85, and vitamin E d-alpha-tocopheryl polyethylene glycol 1000 succinate on P-glycoprotein efflux and enterocyte-based metabolism in excised rat intestine. AAPS PharmSci 2002:4(4):E40.
49. Neuzil J, Weber T, Schroder A, Lu M, Ostermann G, Gellert N, Mayne GC, Olejnicka B, Negre-Salvayre A, Sticha M, Coffey RJ, Weber C. Induction of cancer cell apoptosis by alpha-tocopheryl succinate: molecular pathways and structural requirements. Faseb J 2001:15(2):403-415.
50. Neuzil J, Weber T, Terman A, Weber C, Brunk UT. Vitamin E analogues as inducers of apoptosis: implications for their potential antineoplastic role. Redox Rep 2001:6(3):143-151.
51. Neuzil J, Zhao M, Ostermann G, Sticha M, Gellert N, Weber C, Eaton JW, Brunk UT. Alpha-tocopheryl succinate, an agent with in vivo anti-tumour activity, induces apoptosis by causing lysosomal instability. Biochem J 2002:362(Pt 3):709-715.
52. Yu W, Israel K, Liao QY, Aldaz CM, Sanders BG, Kline K. Vitamin E succinate (VES) induces Fas sensitivity in human breast cancer cells: role for Mr 43,000 Fas in VES-triggered apoptosis. Cancer Res 1999:59(4):953-961.
53. Yu W, Jia L, Wang P, Lawson KA, Simmons-Menchaca M, Park SK, Sun L, Sanders BG, Kline K. In vitro and in vivo evaluation of anticancer actions of natural and synthetic vitamin E forms. Mol Nutr Food Res 2008:52(4):447-456.
54. Neuzil J, Dong LF, Wang XF, Zingg JM. Tocopherol-associated protein-1 accelerates apoptosis induced by alpha-tocopheryl succinate in mesothelioma cells. Biochem Biophys Res Commun 2006:343(4):1113-1117.
55. Feng SS, Mei L, Anitha P, Gan CW, Zhou W. Poly(lactide)-vitamin E derivative/montmorillonite nanoparticle formulations for the oral delivery of Docetaxel. Biomaterials 2009:30(19):3297-3306.
56. Gu X, Schwartz JL, Pang X, Zhou Y, Sirois DA, Sridhar R. Cytotoxicity of liposomal alpha-tocopheryl succinate towards hamster cheek pouch carcinoma (HCPC-1) cells in culture. Cancer Lett 2006:239(2):281-291.
57. Zaki NM, Tirelli N. Gateways for the intracellular access of nanocarriers: a review of receptor-mediated endocytosis mechanisms and of strategies in receptor targeting. Expert Opin Drug Deliv 2010:7(8):895-913.
58. Zhang K, Wang Y, Yu A, Zhang Y, Tang H, Zhu XX. Cholic acid-modified dendritic multimolecular micelles and enhancement of anticancer drug therapeutic efficacy. Bioconjug Chem 2010:21(9):1596-1601.
59. Morgan MT, Nakanishi Y, Kroll DJ, Griset AP, M.A. C, Wathier M, Oberlies NH, Manikumar G, Wani MC, Grinstaff MW. Dendrimer-encapsulated camptothecins: increased solubility, cellular uptake, and cellular retention affords enhanced anticancer activity in vitro. Cancer Res 2006:66(24):11913-11921.
60. Arias JL, Reddy LH, Couvreur P. Polymeric nanoparticulate system augmented the anticancer therapeutic efficacy of gemcitabine. J Drug Target 2009:17(8):586-598.
61. Zhang Z, Feng SS. Self-assembled nanoparticles of poly(lactide)--Vitamin E TPGS copolymers for oral chemotherapy. Int J Pharm 2006:324(2):191-198.
62. You J, Hu FQ, Du YZ, Yuan H, Ye BF. High cytotoxicity and resistant-cell reversal of novel paclitaxel loaded micelles by enhancing the molecular-target delivery of the drug. Nanotechnology 2007:18(49):495101.
63. Dong Y, Feng SS. In vitro and in vivo evaluation of methoxy polyethylene glycol-polylactide (MPEG-PLA) nanoparticles for small-molecule drug chemotherapy. Biomaterials 2007:28(28):4154-4160.